Nondiffusive Transport in Tokamaks: Three-Dimensional Structure of Bursts and the Role of Zonal Flows

P. Beyer and S. Benkadda

Equipe Dynamique des Systèmes Complexes, LPIIM, CNRS–Université de Provence, Centre de St. Jérôme, Case 321, 13397 Marseille Cedex 20, France

X. Garbet

Association Euratom–CEA sur la Fusion, CEA Cadarache, 13108 St-Paul-lez-Durance, France

P. H. Diamond

Department of Physics, University of California at San Diego, La Jolla, California 92093-0319

(Received 20 June 2000)

Large scale transport events are studied in simulations of resistive ballooning turbulence in a tokamak plasma. The spatial structure of the turbulent flux is analyzed, indicating radially elongated structures (streamers) at the low field side which are distorted by magnetic shear at different toroidal positions. The interplay between self-generated zonal flows and transport events is investigated, resulting in significant modifications of the frequency and the amplitude of bursts. The propagation of bursts is studied in the presence of a transport barrier generated by a strong shear flow.

PACS numbers: 52.35.Ra, 52.35.Py, 52.35.Mw

Recently, considerable interest has developed in the role of large scale transport events or bursts in turbulence [1–4]. Radially propagating fronts have been observed in various turbulence simulations [5–9] and on electron temperature fluctuations in tokamak experiments [10]. They might be good candidates to explain fast transients [11]. A single structure of this sort is suggested to be a radially extended, poloidally localized convective cell called a streamer [12,13]. However, the three-dimensional (3D) structure of such a burst has not yet been studied. A different type of strongly anisotropic flow are the so-called zonal flows that are poloidally extended, radially localized flows. The shearing due to zonal flows is the key mechanism that governs the self-regulation and saturation of drift waves [14–16]. On the other hand, the influence of zonal flows on the appearance of bursts has not yet been analyzed in the numerical simulations. Another important question is the effect of a sheared mean flow on these transport events. The main question here is to see if bursts do propagate through a transport barrier that is generated by the velocity shear.

In this Letter, novel results are presented concerning the three points specified above: the 3D structure of bursts, the influence of zonal flows, and the effect of including a velocity shear layer. These results are obtained from qualitative observations of simulations of resistive ballooning turbulence at the plasma edge. The turbulence is driven by a constant incoming flux. The model consists of two equations for the vorticity and pressure, respectively. The normalized form of these equations is [17,18]

$$\frac{d}{dt}\nabla_\perp^2\phi = -\nabla_\parallel^2\phi - Gp + \nu\nabla_\perp^4\phi\,, \qquad (1)$$

$$\frac{dp}{dt} = \chi_\parallel\nabla_\parallel^2 p + \chi_\perp\nabla_\perp^2 p + S\,. \qquad (2)$$

Here $d/dt = \partial/\partial t + \{\phi, \cdot\}$, where the Poisson bracket represents the convection due to the $\vec{E}\times\vec{B}$ flow. Note that the aim of this work is to study basic dynamic processes in 3D turbulence at the plasma edge. Therefore, in this simplified MHD model, diamagnetic effects and magnetic fluctuations are not included. Equations (1) and (2) describe the evolution of the complete fields of potential and pressure, including equilibrium and fluctuations. The magnetic field in toroidal coordinates is $\vec{B}_0 = B_\varphi[\hat{e}_\varphi + r/(Rq)\hat{e}_\theta]$. Normalized slab coordinates are introduced in the vicinity of a reference surface, $x = (r - r_0)/\xi$, $y = r_0\theta/\xi$, $z = R_0\varphi/L_s$, where the perpendicular length scale ξ is typically a few ion Larmor radii and the shear length L_s is of the order of R_0. Detailed descriptions of the normalization, the safety factor $q(x)$, and the toroidal curvature operator G are given in [18]. In the presence of a pressure gradient, the magnetic curvature drives the ballooning instability at the low field side. Expanding the fields ϕ and p into Fourier series in the poloidal (mode number m) and toroidal (n) directions, each Fourier mode is localized in the vicinity of its resonant surface $x = x_{q=m/n}$. The simulation region is restricted to the domain between the $q = 2$ and $q = 3$ surfaces at the plasma edge. Only resonant modes are considered, up to the toroidal mode number $n = 24$ (i.e., 325 modes). In the radial direction, finite differences are used and the fields ϕ and p are extrapolated to zero in two "buffer" zones at the left and the right sides of the interval $[x_{q=2}; x_{q=3}]$, respectively. At the left boundary of the computational domain, $\partial_x p_{(m,n)=(0,0)}$ vanishes (and p_{00} is free). A total number of

 0031-9007/00/85(23)/4892(4)$15.00

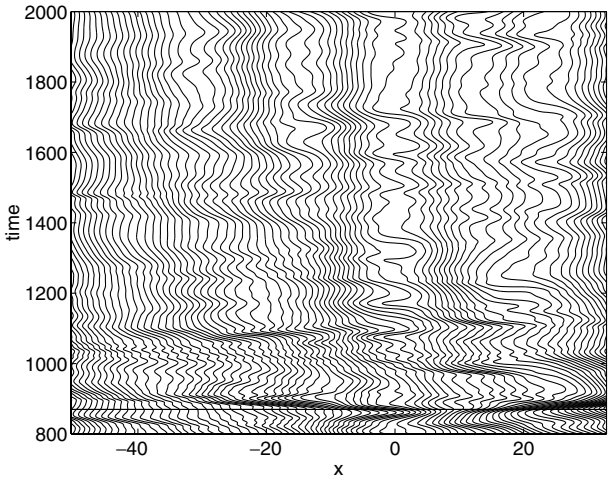

FIG. 1. Time evolution of the magnetic surface averaged pressure profile [isobars in the (x, t) plane]. The horizontal line indicates the time at which Figs. 2 and 3 are taken.

120 grid points are used in the main interval and 2×36 in the buffer regions. The source $S(x)$ is Gaussian shaped and located in the left buffer zone.

The values of the parameters $\nu = \chi_\perp = 2$, $\chi_\parallel = 0.5$, $\xi/r_0 = 0.002$, $L_s/R_0 = 1$, $q_0 = 2.5$, and $[x_{q=2}; x_{q=3}] = [-50; 33.33]$ have been chosen such that in the case of a constant equilibrium pressure gradient of -1 the ballooning modes with wave numbers n in the range considered in the present simulations are all unstable. More precisely, for each wave number n, this is true for the mode with the largest linear growth rate, i.e., those with no knots in the radial envelope. In a linear analysis, the amplitude of the source needed to build up a pressure gradient of -1 would be determined by $\chi_\perp^{-1} \int S\, dx = 1$, where the integral is taken over the left buffer region. However, in the fully nonlinear case, modes react back on the pressure profile and strongly weaken the mean gradient. To counterbalance this effect, the source has to be increased, but it turns out that even for very large amplitudes, the resulting mean pressure gradient is only slightly above the linear instability threshold. However, strong gradients appear locally in space and time. In the present simulations, an amplitude of the source 50 times larger than the value given by the linear expression is used, which is the largest amplitude possible with the given numerical discretization.

Following the time evolution of the radial pressure profile, large bursts are observed alternating with quiet periods, as illustrated in Fig. 1. One observes both low pressure events traveling inward and high pressure bursts propagating in the outward direction. Note that the early times shown in Fig. 1 correspond to a transient phase where the mean pressure gradient has not yet reached a statistically stationary state. In this phase, many large bursts are observed. From the previous plot, it is possible to determine a time when a large burst appears. To investigate the 3D structure of this burst, the spatial distribution

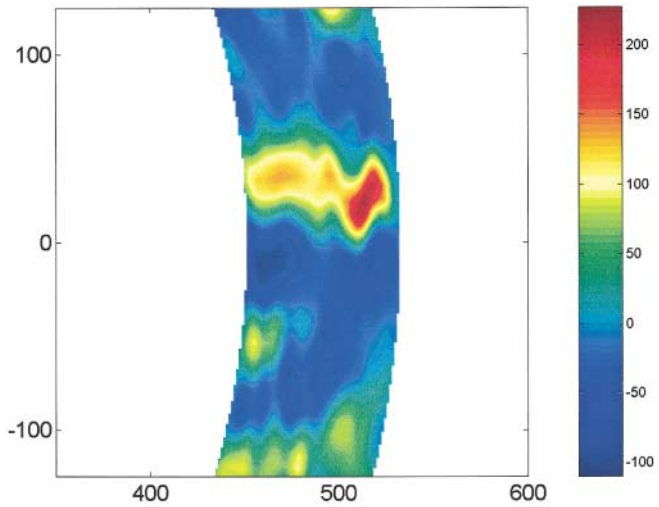

FIG. 2 (color). Radially elongated structure (streamer) of the turbulent radial flux in a section (at the low field side) of a poloidal plane. The coordinates $(r\cos\theta, r\sin\theta)$ in this plane are given in units of the perpendicular scale length ξ.

of the turbulent radial flux is analyzed at that specific time. A dominant structure corresponding to a strong local maximum of the flux is observed. At the low field side, this structure is highly elongated in the radial direction which suggests its interpretation as a streamer. To illustrate this, Fig. 2 shows the contours of the turbulent radial flux in a small section of the poloidal plane, at the toroidal position where the structure passes at the low field side. In the toroidal direction, the maximum of the flux follows the local magnetic field line at each radial position, which results in a strong distortion due to magnetic shear. This indicates that structures and magnetic shear are not incompatible. Since the modulational structure drive has ballooning character, the streamer can adjust to the magnetic shear. Figure 3 shows the structure at a distance

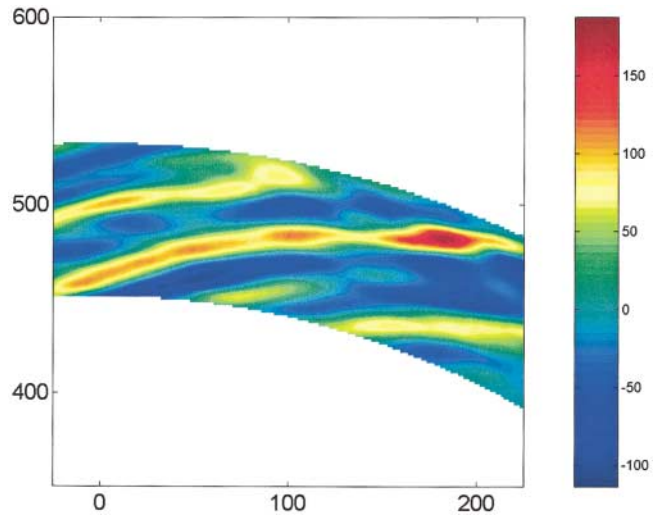

FIG. 3 (color). Same structure as in Fig. 2 one-half turn around the torus away.

corresponding to half a tour around the torus. Note that the amplitude of the flux is lower in this region due to the ballooning character of the turbulence. The corresponding e-folding length in the toroidal direction can be roughly estimated by 2π. To distinguish between a possible linear or nonlinear character of the structure, the toroidal wave number spectrum of the corresponding kinetic energy is calculated. It shows that the streamer is composed of a large ($\sim$10) number of modes with different toroidal wave numbers n and is therefore clearly different from a linear ballooning mode that is characterized by a single wave number n [19]. Therefore, there is strong evidence that the generation of streamers is an intrinsically multimode nonlinear process rather than a secondary instability of a purely linear eigenmode flow.

In the previous simulations, the generation of zonal flows has been artificially suppressed. In order to study the influence of these flows on the large scale transport events, simulations including self-consistently generated zonal flows are performed. As shown in Fig. 4, the frequency of appearance of bursts is found to be remarkably higher compared to the previous case (Fig. 1). On the other hand, the amplitudes of single events are lower. More precisely, the spectrum of the turbulent radial flux at a given radial position exhibits a $1/f$ decrease in a range of intermediate frequencies [3,5,6] up to a certain cutoff, and the latter is extended to higher frequencies when zonal flows are included (Fig. 5). This behavior can be understood analyzing the time evolution of the velocity shear at the same given radial position. When a burst is building up, the velocity shear starts growing after a short time delay, inhibiting the flux to grow to large amplitudes. This is due to the decorrelation of the radially elongated structures by the shear stress. The cross correlation function of the turbulent radial flux and the velocity shear shows a maximum at a time delay of the order of 10 time units. This corresponds roughly to the cutoff in the frequency spectrum mentioned above.

The change in the frequency spectrum is in perfect agreement with the one observed in Ref. [2] in the running sandpile model. There a suppression of the low-frequency components and an increase of the high-frequency parts are observed. Here the simulations presented so far confirm

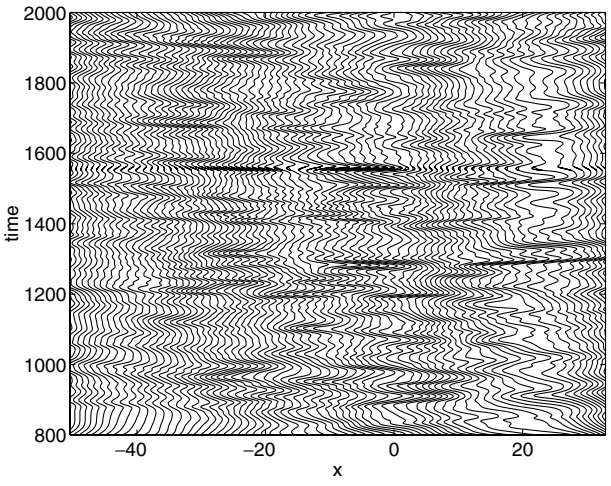

FIG. 4. Time evolution of the magnetic surface averaged pressure profile in the case with self-consistently generated zonal flows.

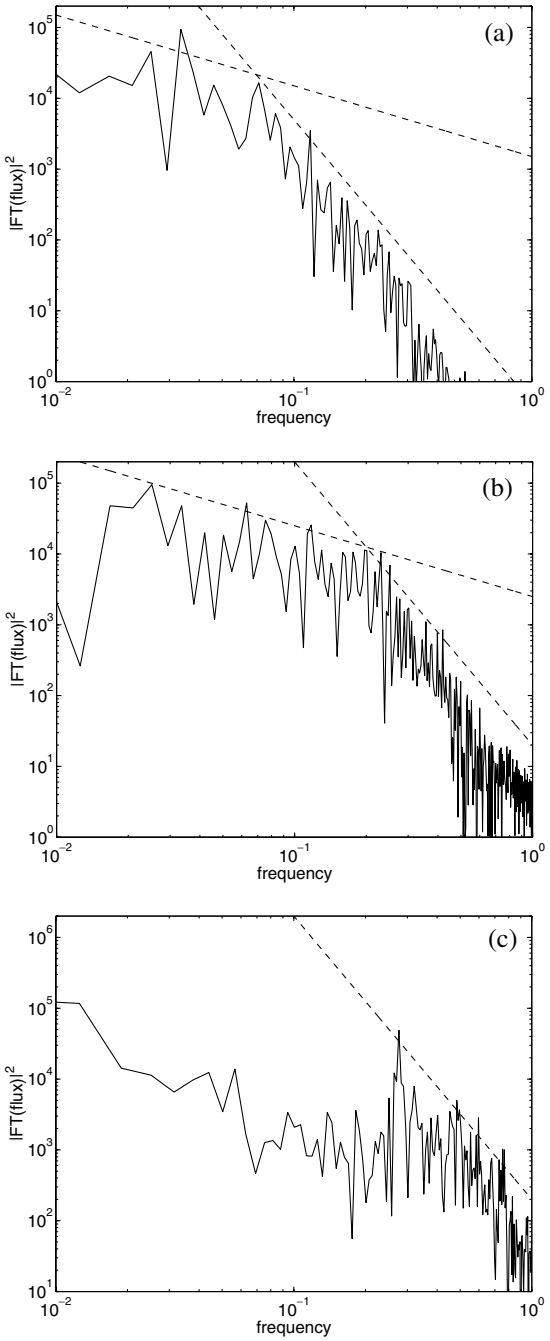

FIG. 5. Frequency spectra of the turbulent radial flux at $x = 0$ in the cases without zonal flows (a), with self-consistent zonal flows (b), and with externally imposed strong shear flow (c). In each case, the spectrum is calculated in the statistically stationary state. Dashed lines indicate slopes of -1 and -4, respectively.

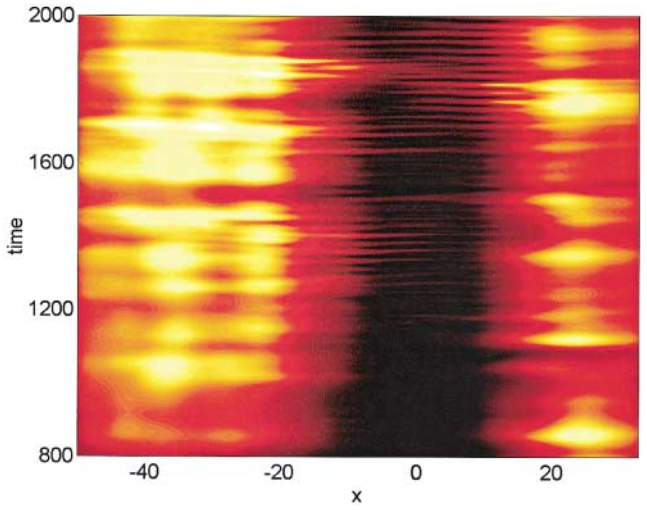

FIG. 6 (color). Time evolution of the magnetic surface averaged turbulent radial flux in the case with externally imposed strong shear flow [minimum $= -0.1$ (black), maximum $= 3.8$ (white)].

the increase at high frequencies in the presence of zonal flows. As will be shown now, the decrease at low frequencies is due to a region with strong mean shear that is investigated in Ref. [2]. Therefore, a third simulation is performed, imposing a sheared equilibrium rotation at the vicinity of the $x = 0$ surface. The velocity shear is 5 times larger than those generated by the turbulence in the previous simulation. In this case, a transport barrier builds up in the shear region, characterized by a strongly reduced turbulent radial flux (Fig. 6). Bursts are still observed in this region, but their amplitudes are very small, and, coming from both sides of the barrier, they almost vanish in the center. However, some perturbations travel through the barrier, as shown by recent simulations [20]. The frequency of appearance of bursts is even higher than in the previous case. In fact, as illustrated in Fig. 5c, the reduction of turbulent transport is found to be due to the suppression of low-frequency components in the turbulent flux. As the time averaged total radial flux is constant, the transport in the barrier region must be approximatively neoclassical. In fact, a large pressure gradient builds up in this region. Note that the character of the bursts inside the barrier is close to that of a quasicoherent oscillation. Concerning the probability distribution function (PDF) of the turbulent flux at a given radial position, one observes that the characteristic width of these functions is larger when zonal flows are included compared to the case without flows. This means that the turbulent flux has inherent statistical properties and, for transport predictions, the PDFs have to be considered rather than only the mean value. However, in the case with strong shear flow, the PDF in the shear region shows a strong narrow peak for low fluxes in combination with a long tail. This is in agreement with the observations in Ref. [2].

In conclusion, the 3D structure of nondiffusive transport events in a tokamak plasma has been studied numerically in a resistive ballooning system. These bursts are found to be highly radially elongated on the low field side and localized along magnetic field lines that cause a distortion of the streamer in the parallel direction. The streamer is found to be generated by an intrinsically nonlinear process. Self-generated zonal flows inhibit the growth of bursts, reducing their amplitude and increasing the frequency of appearance. In the presence of a transport barrier generated by a strong shear flow, the amplitudes of bursts almost vanish in the center of the barrier.

P. B. and S. B. were supported by the Commissariat à l'Energie Atomique, LRC Contract No. DSM 99-14. P. D. was supported by U.S. D.O.E. Grant No. FG03-853275.

[1] P. H. Diamond and T. S. Hahm, Phys. Plasmas **2**, 3640 (1995).
[2] D. E. Newman *et al.,* Phys. Plasmas **3**, 1858 (1996).
[3] B. A. Carreras *et al.,* Phys. Plasmas **3**, 2903 (1996).
[4] J. A. Krommes, Phys. Plasmas **7**, 1752 (2000).
[5] X. Garbet *et al.,* Nucl. Fusion **39**, 2063 (1999).
[6] Y. Sarazin and Ph. Ghendrih, Phys. Plasmas **5**, 4214 (1998).
[7] P. Beyer *et al.,* Plasma Phys. Controlled Fusion **41**, A757 (1999).
[8] S. Benkadda *et al.,* Phys. Scr. **T84**, 14 (2000).
[9] F. Jenko, W. Dorland, and M. Kotschenreuther, Phys. Plasmas **7**, 1904 (2000).
[10] P. A. Politzer, Phys. Rev. Lett. **84**, 1192 (2000).
[11] Y. Sarazin *et al.,* Phys. Plasmas **7**, 1085 (2000).
[12] S. Champeaux and P. H. Diamond (to be published).
[13] J. F. Drake, P. N. Guzdar, and A. B. Hassam, Phys. Rev. Lett. **61**, 2205 (1988).
[14] Z. Lin *et al.,* Phys. Rev. Lett. **83**, 3645 (1999).
[15] P. H. Diamond *et al.,* in *Proceedings of the 17th IAEA Fusion Energy Conference, Yokohama, Japan, 1998* (IAEA, Vienna, 1998).
[16] A. M. Dimits *et al.,* Phys. Plasmas **7**, 969 (2000).
[17] P. Beyer and K. H. Spatschek, Phys. Plasmas **3**, 995 (1996).
[18] P. Beyer, X. Garbet, and P. Ghendrih, Phys. Plasmas **5**, 4271 (1998).
[19] P. Beyer, S. Benkadda, and X. Garbet, Phys. Rev. E **61**, 813 (2000).
[20] Y. Sarazin *et al.,* in *Proceedings of the 27th EPS Conference on Controlled Fusion and Plasma Physics, Budapest, Hungary, 2000* (EPS, Petit-Lancy, 2000).